Published in final edited form as:
J Diabetes. 2010 December ; 2(4): 267–274. doi:10.1111/j.1753-0407.2010.00088.x.

Macrophage Migration Inhibitory Factor Deficiency Augments Cardiac Dysfunction in Type 1 Diabetic Murine Cardiomyocytes

Chao Tong[1], **Alex Morrison**[1], **Xiaoyan Yan**[1], **Peng Zhao**[2], **Eddie D Yeung**[1], **Jingying Wang**[1], **Jianxin Xie**[3], and **Ji Li**[1,3]

[1]Department of Pharmacology and Toxicology, SUNY University at Buffalo, Buffalo, NY 14214, USA

[2]Department of Cardiology, Shandong Provincial Hospital, Shandong University, Jinan, 250021

[3]School of Medicine, Shihezi University, Shihezi, P.R. China

Abstract

Background—It has become evident that macrophage migration inhibitory factory (MIF) is associated with the development of type 1 diabetes. The objective of this study is to determine whether MIF plays a role in cardiac contractile dysfunction of type 1 diabetic mice.

Methods—Mechanical and intracellular Ca^{2+} properties were measured in cardiomyocytes isolated from wild type (WT) and MIF knock out (MIF KO) mice administrated with or without STZ (200mg/kg, i.p.). The relative stress signaling was evaluated using Western blots analysis.

Results—STZ-induced diabetic mellitus depressed peak shortening (PS), maximal velocity of shortening/relengthening (±dL/dt) and prolonged duration of relengthening (TR90) of both WT and MIF KO cardiomyocytes ($p<0.01$ *vs.* WT and MIF control, respectively), which might be associated with the reduced intracellular Ca^{2+} decay in both groups. However, WT-STZ cardiomyocytes demonstrated significantly better contractile functions and intracellular Ca^{2+} properties compared to MIF KO-STZ group (all $p<0.05$ *vs.* WT-STZ, respectively). Interestingly, the physiological data clearly showed that the blood glucose levels of MIF KO-STZ group were significantly higher than that of WT-STZ group ($p<0.01$ *vs.* WT-STZ group, respectively). Moreover, the phosphorylation levels of AMPK and its direct downstream target acetyl-CoA carboxylase (ACC) in MIF KO-STZ hearts were markedly lower than that in WT-STZ hearts ($p<0.05$ *vs.* WT-STZ, respectively), while there were no significant difference between WT and MIF KO control groups.

Conclusions—There is a beneficial action of MIF in the management of cardiac dysfunction under type 1 diabetes. The cardioprotection effect of MIF might be associated with AMPK signaling.

Keywords

macrophage migration inhibitory factor; type 1 diabetes; cardiomyocytes

Correspondence to: Ji Li, PhD, Department of Pharmacology and Toxicology, SUNY University at Buffalo, Buffalo, NY 14214; Tel: 716-829-5711; Fax: 716-829-2801; jli23@buffalo.edu.

Disclosure
The authors have nothing to declare.

Introduction

Type 1 diabetes mellitus (T1D) is a multifactorial disorder caused by the lack of endogenous insulin. It is a consequence of an immune attack mediated by auto reactive T cells and macrophages against pancreatic β-cells. Type 1 diabetes afflicts approximately four million people in North America and epidemiological data concur that the incidence and prevalence of T1D are increasing world widely.[1] Although immune system plays a key role in pathogenesis of T1D, current studies have much focused on identifying inimmunotherapeutical approaches that could halt or delay β-cell destruction in prediabetic individuals or those patients in early phase of T1D. Streptozotocin (STZ) is a natural chemical that has selectively toxicity for pancreatic beta cells (β-cells). β-cells are responsible for secretion of insulin - a hormone that maintains blood glucose homeostasis. Lack of insulin associated with the destruction of β-cells links STZ to T1D. Based on above mechanism, STZ is commonly used in animal research to study the pathogenesis and influence of T1D in mouse.

Macrophage migration inhibitory factor (MIF) was originally discovered as a lymphokine that was derived from activated T-cells; it inhibits the random migration of macrophages *in vitro* and regulates T-cell activation as well as proliferation.2 Currently, accumulating evidences show that MIF plays a key role in acute and chronic inflammatory diseases such as septic shock,3 rheumatoid arthritis,4 and inflammatory lung diseases.[5] Intriguingly, we recently unveiled the cardioprotection role of MIF in the heart during ischemia/reperfusion via modulating AMP-activated protein kinase (AMPK) signaling pathway.[6]

AMPK has been found to be a key defender against cardiovascular diseases and cellular stress.7–9 Activation of AMPK regulates transport and metabolism of blood glucose and fatty acids to attenuate harms for heart, while synthesizes energy molecule ATP that is beneficial for maintaining normal cellular function.10, 11 Another kniase signaling called mitogen-activated protein kinases (MAPKs) also play important role in the heart during cellular stress,[12] it is composed of three major subgroups: extracellular signal-regulated kinase (ERK), p38 mitogen-activated protein kinases (p38 MAPK) and c-Jun N-terminal kinases (JNK). There are evidence that activation of MAPK family regulates various cellular activities, such as repair and apoptosis, in the heart.12, 13

In this study, our hypothesis is that MIF may play a beneficial role for heart under STZ induced T1D. We found that hyperglycemia and much more body weight lost were observed in MIF KO mice after 14 days of STZ injection, and STZ-induced T1D leads to cardiac contractile dysfunction in both WT and MIF KO mice but MIF KO demonstrated intolerance versus WT cardimyocytes.

Materials and Methods

Experimental diabetic animals

The experimental procedure was approved by the Institutional Animal Use and Care Committees (IACUC) in University at Buffalo-SUNY. All animal procedures were in accordance with NIH animal care standards. T1D animal model will be generated as previously described.[14] In brief, eight to ten week-old weight-matched male wild type (WT, FVB/NJ) and MIF KO (FVB/NJ background) mice were given a single injection of streptozotocin (STZ, 200 mg/kg., i.p.). Fasting blood glucose levels were evaluated 14 days later. A supplemental STZ injection at 100 mg/kg (i.p.) was given if the fasting blood glucose was below 12 mM. All diabetic mice (fasting blood glucose level >12 mM) were maintained for a total of 2 weeks (after confirming diabetes) with free access to standard lab chow and tap water.

Isolation of cardiomyocytes

Hearts were rapidly removed from anesthetized mice and immediately mounted on a temperature-controlled (37°C) Langendorff perfusion system as described previously.[9] After perfusion with modified Tyrode solution (Ca^{2+} free) for 2 min, the heart was digested for 10 min with Liberase Blendzyme 4 (Hoffmann-La Roche Inc., Indianapolis, IN, USA) in modified Tyrode solution (NaCl 135 mM, KCl 4.0 mM, $MgCl_2$ 1.0 mM, HEPES 10 mM, NaH_2PO_4 0.33 mM, glucose 10 mM, butanedione monoxime 10 mM). The digested heart was then removed from the cannula and the left ventricle was cut into small pieces, which were gently agitated and the pellet of cells was resuspended and allowed to settle for another 20 min at room temperature during which time extracellular Ca^{2+} was added incrementally back to 1.25 mM. Cell viability was approximately 75% in all four animal groups.

Cell shortening/relengthening measurement

The mechanical properties of cardiomyocytes were assessed using a SoftEdge MyoCam system (IonOptix Corporation, Milton, MA, USA).[9] In brief, left ventricular cardiomyocytes were placed in a chamber mounted on the stage of an inverted microscope (Motic AE31) and superfused at 25°C with a buffer (NaCl 131 mM, KCl 4 mM, $CaCl_2$ 1 mM, $MgCl_2$ 1 mM, Glucose 10 mM and HEPES 10 mM, pH 7.4). The cells were field stimulated with suprathreshold voltage at a frequency of 0.5 Hz.9 The IonOptix SoftEdge was used to capture changes in cell length during shortening and relengthening. Cell shortening and relengthening were assessed using the following indices: peak shortening (PS) - indicative of peak ventricular contractility; and maximal velocities of shortening/relengthening (±dL/dt) - indicatives of maximal velocities of ventricular pressure increase/decrease.

Intracellular Ca^{2+} measurement

Myocytes were loaded with fura-2/AM and fluorescence measurements were recorded with a dual-excitation fluorescence photo multiplier system (IonOptix) as described previously.[15] Briefly, myocytes were placed on an Motic AE31 inverted microscope and imaged through a Fluor 40x oil objective. Cells were exposed to light emitted by a 75 W lamp and passed through either a 360 or a 380 nm filter, while being stimulated to contract at 0.5 Hz. Fluorescence emissions were detected between 480 and 520 nm by a photomultiplier tube after first illuminating the cells at 360 nm for 0.5 s then at 380 nm for the duration of the recording protocol (333 Hz sampling rate). The 360 nm excitation scan was repeated at the end of the protocol and qualitative changes in intracellular Ca^{2+} concentration were inferred from the ratio of fura-2 fluorescence intensity (FFI) at two wavelengths (360/380). Fluorescence decay time was measured as an indication of the intracellular Ca^{2+} clearing rate. Both single and bi-exponential curve fit programs were applied to calculate the intracellular Ca^{2+} decay constant.

Western blot analysis

The total protein was prepared after treatment. In brief, left ventricles were rapidly removed and homogenized in a lysis buffer containing 20 mM Tris (pH 7.4), 150 mM NaCl, 1 mM EDTA, 1 mM EGTA, 1% Triton, 0.1% SDS, and 1% protease inhibitor cocktail. The protein concentration of the supernatant was evaluated using the protein assay reagent (Bio-Rad, Hercules, CA). Equivalent (30μg protein/lane) protein and prestained molecular weight marker (GIBCO, Gaithersburg, MD) were loaded onto each well of 7%~15% SDS-polyacrylamide gels in a minigel apparatus (Mini-PROTEAN II, Bio-Rad), electrophoresis at 90V for 90min, and then transferred to nitrocellulose membranes (0.2 μm pore size, Bio-Rad). Membranes were incubated for 1h in a blocking solution containing 5% nonfat milk in TBS-T before being rinsed in TBS-T and incubated overnight at 4°C with anti-ERK (Santa Cruz Biotech, Santa Cruz, CA), anti-phospho-ERK (p-ERK, Santa Cruz), anti-JNK (Cell

Signaling Tech, Beverly, MA), anti-phospho-JNK (p-JNK, Cell Signaling), anti-p38 (Cell Signaling), and anti-phospho-p38(p-p38, Cell Signaling), Anti-phospho-AMPK (Cell Signaling), Anti-AMPK(Cell Signaling), Anti-Phospho-Acetyl-CoA Carboxylase (p-ACC) (Upstate Biotech, Lake Placid, NY), Anti -Acetyl-CoA Carboxylase (ACC) (Cell Signaling). The intensity of bands was measured with a scanning densitometer (model GS-800; Bio-Rad) coupled with Bio-Rad personal computer analysis software.

Statistical analysis

Data were Mean ± SEM. Differences between groups was assessed using analysis of variance (ANOVA) followed by Newman-Keuls *post hoc* test. A p value less than 0.05 was considered statistically significant.

Results

Intolerance of MIF KO mice on STZ-induced type 1 diabetes

To investigate the role of MIF in STZ-induced type 1 diabetes (T1D), we determined the survival rate of STZ-induced T1D model in both wild type (WT) and MIF KO mice. As shown in survival curve of Fig. 1, the MIF KO mice are more sensitive to STZ-induced T1D compared to counterpart WT mice, which suggest that MIF play a role in keeping resistance to STZ-induced type 1 diabetes.

Physiological findings of STZ-induced diabetes

Both WT and MIF KO mice showed hyperglycemia after STZ injection, and there is no significant difference regarding glucose levels between WT and MIF KO mice after 14 days of STZ injection (Fig 2A). However, MIF KO mice lost more body weight after STZ injection compared to WT mice (Fig 2B). The ratio of heart weight to body weight in both WT and MIF KO mice remained similar before and after STZ injection (Fig. 2C).

Mechanical and intracellular Ca^{2+} properties of cardiomyocytes

Mechanical properties were obtained under extracellular Ca^{2+} of 1.0 mM and a stimulus frequency of 0.5 Hz. The results demonstrated that resting cell length was similar in cardiomyocytes from both WT and MIF KO hearts (Fig. 3A), moreover, cardiomyocytes from WT-STZ and MIF KO-STZ groups displayed significantly reduced peak shortening (PS, Fig. 3B) and maximal velocity of shortening/ relengthening (±dL/dt) compared with cardiomyocytes from control groups (Fig. 3C and 3D). MIF KO-STZ cardiomyocytes demonstrated exacerbated dysfunction compared to WT-STZ group (Fig. 3B, 3C and 3D), which indicate that MIF may play cardioprotective function during STZ-induced diabetes symptom.

To explore the potential mechanism(s) involved in the role of MIF protection against T1D induced cardiomyocyte contractile defect, intracellular Ca^{2+} homeostasis was evaluated by fluorescent dye fura-2.[9] Our results showed that reduced intracellular Ca^{2+} clearing rate (both single and bi-exponential decays, Fig. 4C and 4D) associated with unchanged resting and electrically stimulated elevation in intracellular Ca^{2+} levels in the cardiomyocytes (Fig. 4A and 4B). Intriguingly, MIF KO-STZ cardiomyocytes demonstrated slower Ca^{2+} clearing rate than WT-STZ cardiomyocytes, even though there is no significant difference between WT-Con and MIF KO-Con groups (Fig. 4). Together, these data suggest that a beneficial role of MIF in T1D associated cardiac dysfunction.

Signaling pathways in the heart during STZ-induced T1D

To understand the molecular mechanisms of MIF beneficial role in the heart during STZ-induced T1D, three cardioprotective signaling pathways were assessed by immunoblotting. The data clearly demonstrated that STZ dramatically stimulated Akt activation in the WT heart (Fig. 5), but not in MIF KO heart (Fig. 5). Because the cardiac Akt activation levels are up-regulated in the MIF KO non-STZ hearts compared to WT non-STZ hearts (Fig. 5), the capacity of Akt signaling response to STZ treatment in the MIF KO hearts may be decreased. Similarly, STZ treatment activates cardiac ERK signaling in the WT heart but not in MIF KO heart (Fig. 6). Furthermore, the cardioprotective signaling, AMPK, was also significantly triggered by STZ in the WT heart, while there is no response to STZ treatment in the MIF KO heart (Fig. 7).

Discussion

We successfully established STZ-induced type 1 diabetes (T1D) model in both FVB WT and MIF KO mice. Blood glucose levels and body weight lost were monitored at day 0 and day 14. The results showed that the blood glucose levels of WT-STZ and MIF KO-STZ mice at day 14 are much higher than that in day 0. Interestingly, at day 14, MIF KO-STZ mice had much more weight loss versus WT-STZ mice, while there is no significantly difference in the ratio of heart weight to body weight (HW/BW). It indicates that *MIF* gene deletion can augment the body weight loss of T1D mouse, even though the general phenotype is similar. There is evidence has depicted dysregulation of cardiac function in T1D.[16] Our results also revealed reduced peak shorting (PS) and maximal velocities of shortening/relengthening (±dL/dt) in both WT-STZ and MIF KO-STZ murine cardiomyocytes, which support that T1D may cause cardiac dysfunctions. The data demonstrate that *MIF* gene knockout exacerbates T1D-induced cardiac contractile dysfunctions, the fact that MIF itself did not affect cardiomyocyte contractile functions, intracellular Ca^{2+} properties and other biochemical makers in non-STZ treated mouse hearts strongly suggest that MIF is not intrinsically harmful to cardiac function.

The AMP-activated protein kinase (AMPK) is an energy-sensing enzyme that can be activated by acute increases in the cellular AMP/ATP ratio.[17,] 18 AMPK mediates several metabolic changes such as decreasing fatty acid and cholesterol synthesis, inhibiting hepatic glucose production, and increasing fatty acid oxidation and muscle glucose uptake.19 In cardiac muscle, AMPK activity is increased by stimuli such as exercise, hypoxia, ischemia, and stress. 17, [18] AMPK plays a pivotal role in monitoring the cellular energy status and regulating energy production and consumption. [19] In present study, we found that STZ-induced T1D triggered this cardioprotective signaling pathway in WT-heart but not in MIF KO heart, it suggests that MIF may mediate the cardiac AMPK adaptive signaling during STZ-induced T1D. Similarly, cardioprotective Akt signaling is also significantly blunted in the MIF KO heart in response to STZ treatment. The higher basal level Akt activation in MIF KO heart versus wild type heart may be attributed to defect inflammatory response in MIF KO mice.[20]

Mitogen-activated protein kinases (MAPKs) are a family of serine-threonine kinases that play a key role in many cellular processes regulating cytoplasmatic activities and gene expression.[21,] 22 Three members of the MAPK family are: ERK, JNK and p38 MAPK. There is mounting evidence that cardiac ERK signaling is mediated protection against various stress in the heart.23 We have reported the signaling cascades of MIF-ERK during stress condition24, the present study revealed for the first time that cardiac ERK signaling in response to T1D is significantly blunted in the MIF KO heart, which support the critical adaptive role of MIF-ERK signaling cascades in the heart.

In conclusion, our study revealed that in Type 1 diabetic murine cardiomyocyte, MIF play an important role in mediating cardioprotective signaling pathways such as AMPK, Akt and ERK. These data provide a strategy for potentially using MIF or MIF agonists in clinical treatment of type 1 diabetes-associated cardiac dysfunction.

Significant finding (s) of the study

Increasing evidence suggests that MIF controls metabolic processes underlying the development of glucose homeostasis under stress. This study for the first time indicate that MIF-AMPK signaling cascade plays a critical role in preventing cardiac dysfunction of type 1 diabetes.

The study adds

AMPK signaling pathway can be a potential target for developing drugs to ameliorate cardiac dysfunction of type 1 diabetes.

Acknowledgments

This study was supported by a Pilot Grant from NIH INBRE 5P20RR016474, American Heart Association (AHA) National SDG0835168N, American Heart Association (AHA) Pre-doctoral Fellowship 10PRE4190043, American Federation for Aging Research (AFAR) 08007, and a pilot grant of 1UL1RR025014-01 from the National Center for Research Resources (NCRR).

References

1. Cvetkovic I, Al-Abed Y, Miljkovic D, Maksimovic-Ivanic D, Roth J, Bacher M, Lan HY, Nicoletti F, Stosic-Grujicic S. Critical role of macrophage migration inhibitory factor activity in experimental autoimmune diabetes. Endocrinology. 2005; 146:2942–2951. [PubMed: 15790730]
2. Bacher M, Metz CN, Calandra T, Mayer K, Chesney J, Lohoff M, Gemsa D, Donnelly T, Bucala R. An essential regulatory role for macrophage migration inhibitory factor in T-cell activation. Proc Natl Acad Sci U S A. 1996; 93:7849–7854. [PubMed: 8755565]
3. Calandra T, Echtenacher B, Roy DL, Pugin J, Metz CN, Hultner L, Heumann D, Mannel D, Bucala R, Glauser MP. Protection from septic shock by neutralization of macrophage migration inhibitory factor. Nat Med. 2000; 6:164–170. [PubMed: 10655104]
4. Morand EF, Leech M, Weedon H, Metz C, Bucala R, Smith MD. Macrophage migration inhibitory factor in rheumatoid arthritis: clinical correlations. Rheumatology (Oxford). 2002; 41:558–562. [PubMed: 12011381]
5. Mizue Y, Ghani S, Leng L, McDonald C, Kong P, Baugh J, Lane SJ, Craft J, Nishihira J, Donnelly SC, Zhu Z, Bucala R. Role for macrophage migration inhibitory factor in asthma. Proc Natl Acad Sci U S A. 2005; 102:14410–14415. [PubMed: 16186482]
6. Miller EJ, Li J, Leng L, McDonald C, Atsumi T, Bucala R, Young LH. Macrophage migration inhibitory factor stimulates AMP-activated protein kinase in the ischaemic heart. Nature. 2008; 451:578–582. [PubMed: 18235500]
7. Russell RR 3rd, Li J, Coven DL, Pypaert M, Zechner C, Palmeri M, Giordano FJ, Mu J, Birnbaum MJ, Young LH. AMP-activated protein kinase mediates ischemic glucose uptake and prevents postischemic cardiac dysfunction, apoptosis, and injury. J Clin Invest. 2004; 114:495–503. [PubMed: 15314686]
8. Zhao P, Wang J, Ma H, Xiao Y, He L, Tong C, Wang Z, Zheng Q, Dolence EK, Nair S, Ren J, Li J. A newly synthetic chromium complex-Chromium (d-phenylalanine)(3) activates AMP-activated protein kinase and stimulates glucose transport. Biochem Pharmacol. 2009; 77:1002–1010. [PubMed: 19073152]
9. Zhao P, Wang J, He L, Ma H, Zhang X, Zhu X, Dolence EK, Ren J, Li J. Deficiency in TLR4 signal transduction ameliorates cardiac injury and cardiomyocyte contractile dysfunction during ischemia. J Cell Mol Med. 2009; 13:1513–1525. [PubMed: 19508385]

10. Young LH. AMP-activated protein kinase conducts the ischemic stress response orchestra. Circulation. 2008; 117:832–840. [PubMed: 18268160]
11. Young LH. A crystallized view of AMPK activation. Cell Metab. 2009; 10:5–6. [PubMed: 19583947]
12. Li J, Miller EJ, Ninomiya-Tsuji J, Russell RR 3rd, Young LH. AMP-activated protein kinase activates p38 mitogen-activated protein kinase by increasing recruitment of p38 MAPK to TAB1 in the ischemic heart. Circ Res. 2005; 97:872–879. [PubMed: 16179588]
13. Liang Q, Elson AC, Gerdes AM. p38 MAP kinase activity is correlated with angiotensin II type 1 receptor blocker-induced left ventricular reverse remodeling in spontaneously hypertensive heart failure rats. J Card Fail. 2006; 12:479–486. [PubMed: 16911916]
14. Wold LE, Ceylan-Isik AF, Fang CX, Yang X, Li SY, Sreejayan N, Privratsky JR, Ren J. Metallothionein alleviates cardiac dysfunction in streptozotocin-induced diabetes: role of $Ca2_+$ cycling proteins, NADPH oxidase, poly(ADP-Ribose) polymerase and myosin heavy chain isozyme. Free Radic Biol Med. 2006; 40:1419–1429. [PubMed: 16631532]
15. Ceylan-Isik AF, Zhao P, Zhang B, Xiao X, Su G, Ren J. Cardiac overexpression of metallothionein rescues cardiac contractile dysfunction and endoplasmic reticulum stress but not autophagy in sepsis. J Mol Cell Cardiol. 2010; 48:367–378. [PubMed: 19914257]
16. Turdi S, Li Q, Lopez FL, Ren J. Catalase alleviates cardiomyocyte dysfunction in diabetes: role of Akt, Forkhead transcriptional factor and silent information regulator 2. Life Sci. 2007; 81:895–905. [PubMed: 17765928]
17. Wang J, Li J. Activated protein C: a potential cardioprotective factor against ischemic injury during ischemia/reperfusion. Am J Transl Res. 2009; 1:381–392. [PubMed: 19956450]
18. Young LH, Li J, Baron SJ, Russell RR. AMP-activated protein kinase: a key stress signaling pathway in the heart. Trends Cardiovasc Med. 2005; 15:110–118. [PubMed: 16039971]
19. Hardie DG. Role of AMP-activated protein kinase in the metabolic syndrome and in heart disease. FEBS Lett. 2008; 582:81–89. [PubMed: 18022388]
20. Verschuren L, Kooistra T, Bernhagen J, Voshol PJ, Ouwens DM, van Erk M, de Vries-van der Weij J, Leng L, van Bockel JH, van Dijk KW, Fingerle-Rowson G, Bucala R, Kleemann R. MIF deficiency reduces chronic inflammation in white adipose tissue and impairs the development of insulin resistance, glucose intolerance, and associated atherosclerotic disease. Circ Res. 2009; 105:99–107. [PubMed: 19478200]
21. Finkel T, Holbrook NJ. Oxidants, oxidative stress and the biology of ageing. Nature. 2000; 408:239–247. [PubMed: 11089981]
22. Li J, Holbrook NJ. Common mechanisms for declines in oxidative stress tolerance and proliferation with aging. Free Radic Biol Med. 2003; 35:292–299. [PubMed: 12885591]
23. Lecour S. Activation of the protective Survivor Activating Factor Enhancement (SAFE) pathway against reperfusion injury: Does it go beyond the RISK pathway? J Mol Cell Cardiol. 2009; 47:32–40. [PubMed: 19344728]
24. Shi X, Leng L, Wang T, Wang W, Du X, Li J, McDonald C, Chen Z, Murphy JW, Lolis E, Noble P, Knudson W, Bucala R. CD44 is the signaling component of the macrophage migration inhibitory factor-CD74 receptor complex. Immunity. 2006; 25:595–606. [PubMed: 17045821]

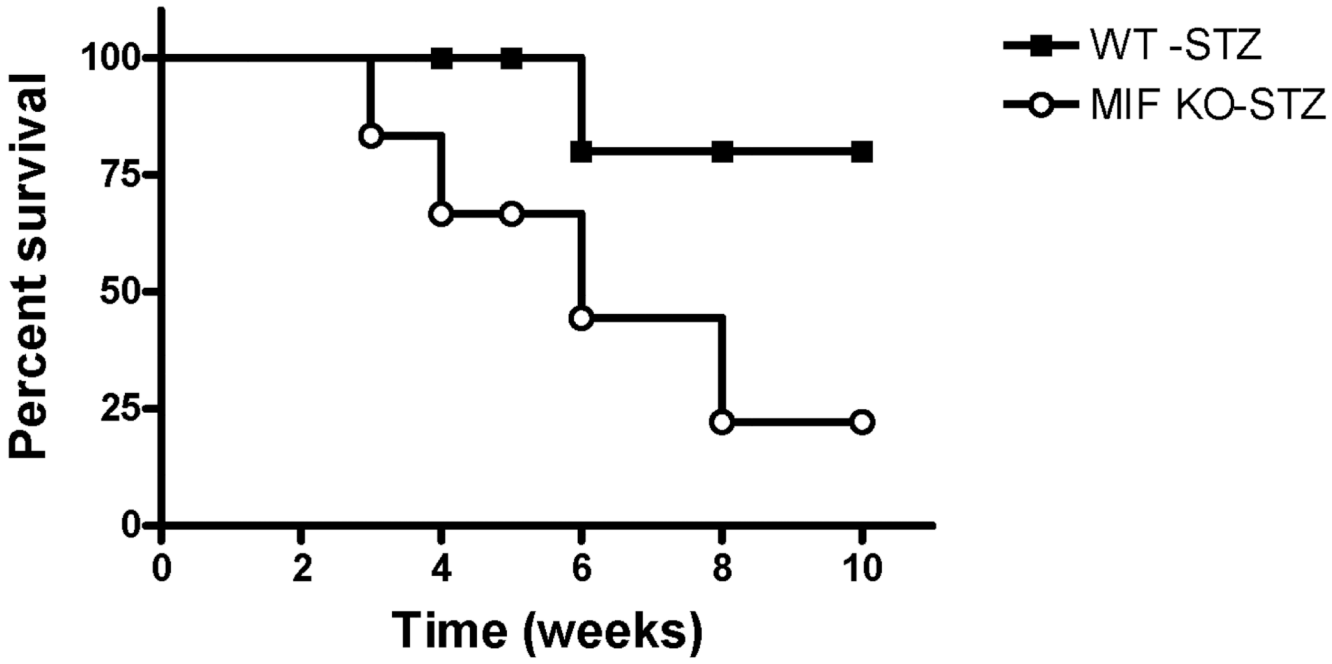

Figure 1.
The survival curve of wild type (WT) and MIF KO mice treated by STZ. Eight to ten week-old weight-matched male wild type (WT, FVB/NJ) and MIF KO (FVB/NJ background) mice were given a single injection of streptozotocin (STZ, 200 mg/kg., i.p.) dissolved in sterile citrate buffer (0.05 M sodium citrate, pH 4.5). A Kaplan-Meier survival curve is shown.

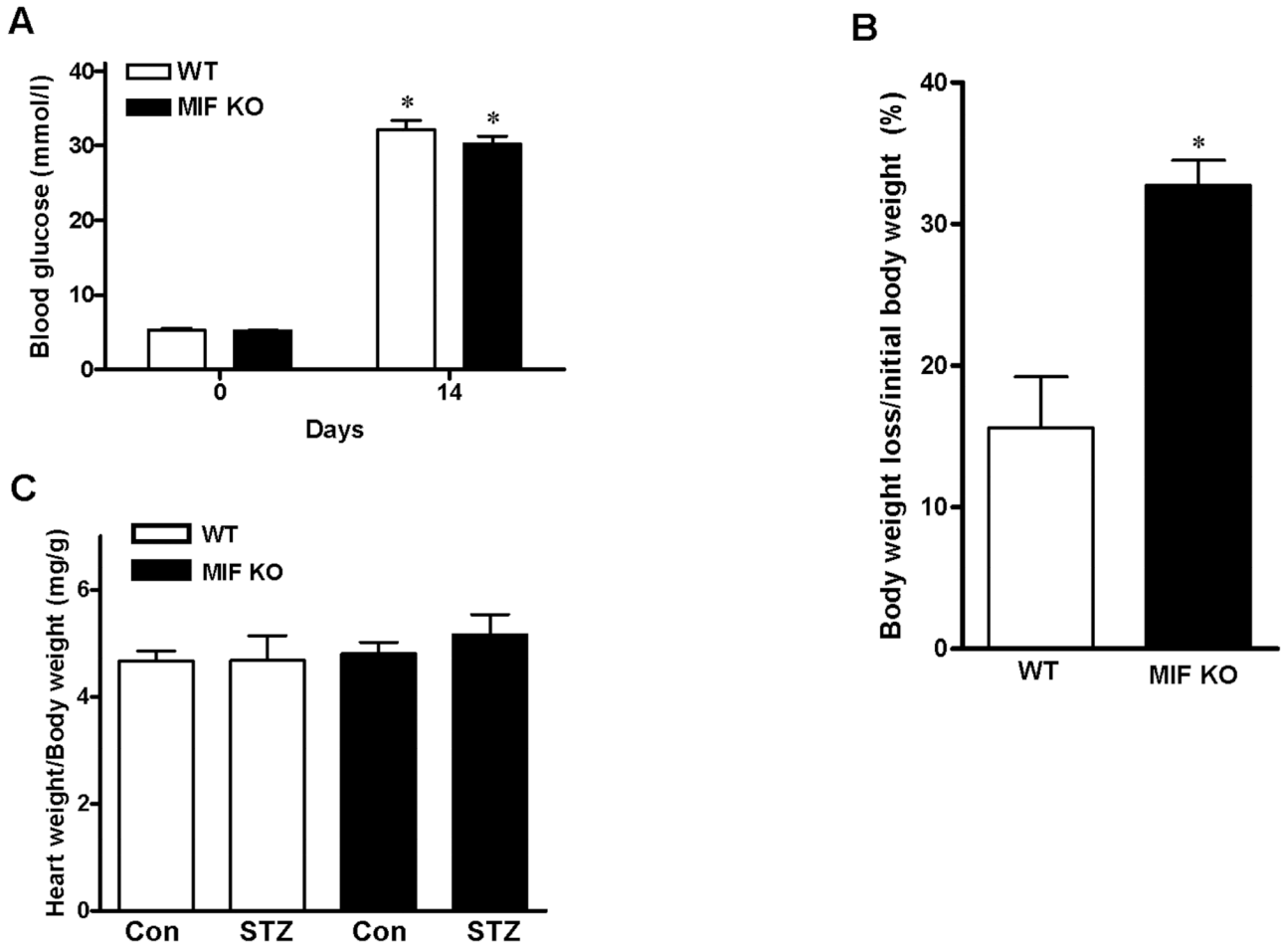

Figure 2.

A. Blood glucose levels were determined at day 0 and day 14 after treatment with STZ. Mean ± SEM, n = 4–5 mice per group, *p < 0.05 *vs.* day 0. **B**. Percentage of body weight loss after STZ injection in WT and MIF KO mice. Mean ± SEM, n = 4–5 mice per group, *p < 0.05 *vs.* WT group. **C**. The ratio of heart weight to body weight. Mean ± SEM; n = 4–5 mice per group.

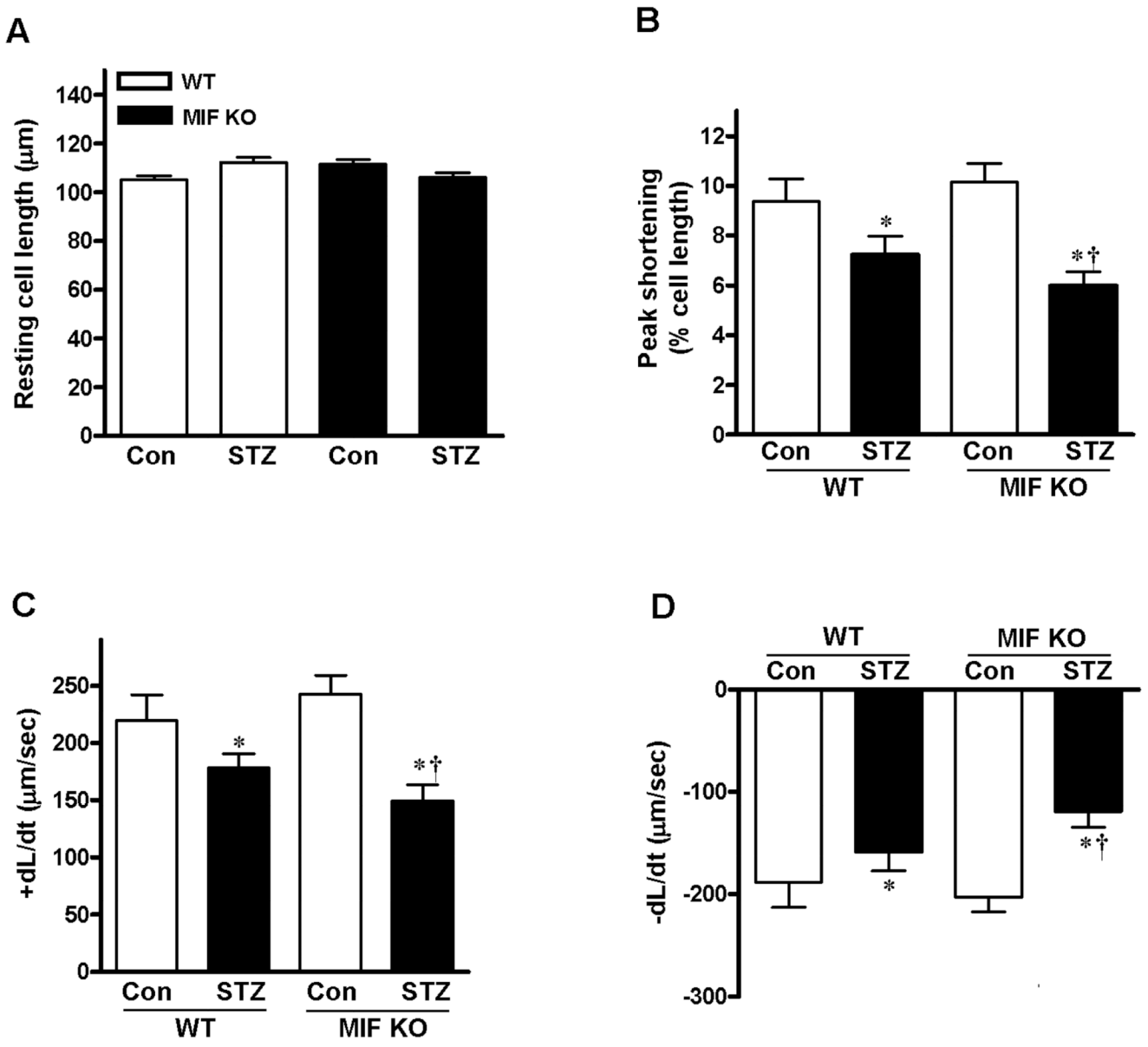

Figure 3.

Contractile properties of cardiomyocytes from WT and MIF KO mice treated with or without STZ (200 mg/kg, i.p.). **A**. Resting cell length; **B**. Peak shortening (PS, normalized to resting cell length); **C**. Maximal velocity of shortening (+dL/dt); **D**. Maximal velocity of relengthening (−dL/dt). Mean ± SEM, n = 50–60 cells per group from 4 mice in each group, *$p < 0.05$ *vs.* control group, respectively; †$p < 0.05$ *vs.* WT-STZ group.

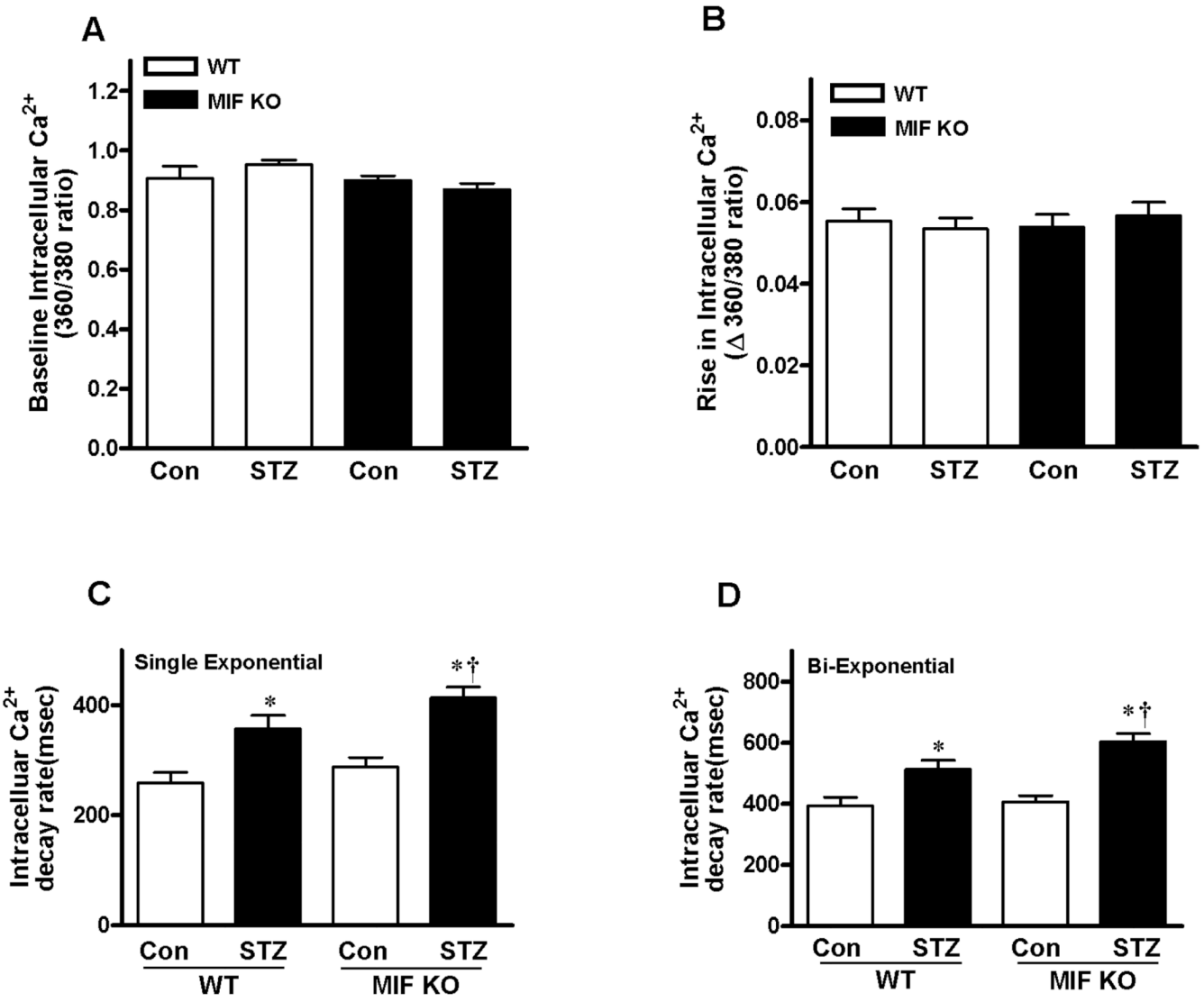

Figure 4.

Intracellular Ca^{2+} transient properties of cardiomyocytes from WT and MIF KO mice treated with or without STZ (200 mg/kg, i.p.). **A**. Resting fura-2 fluorescence intensity (FFI); **B**. Electrically stimulated change in fura-fluorescence intensity (ΔFFI); **C** and **D**. Single and bi-exponential intracellular Ca^{2+} transient decay rate. Mean ± SEM, n = 60–80 cells per group from 3 mice in each group, *p <0.05 *vs.* control group, respectively; †p<0.05 *vs.* WT-STZ group.

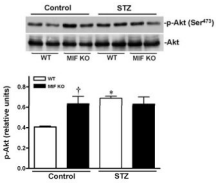

Figure 5.

Cardaic Akt signaling stimulated by STZ-induced T1D. Left ventricles from WT and MIF KO mice treated with or without STZ (200 mg/kg, i.p.) were used for making homogenates. Representative immunoblots of p-Akt (Ser473) and total Akt (upper panel), bars show the relative level of p-Akt in the hearts (lower panel). Mean ± SEM; n =4 samples per group, *p < 0.05 *vs.* control group, respectively; †p < 0.05 *vs.* WT control.

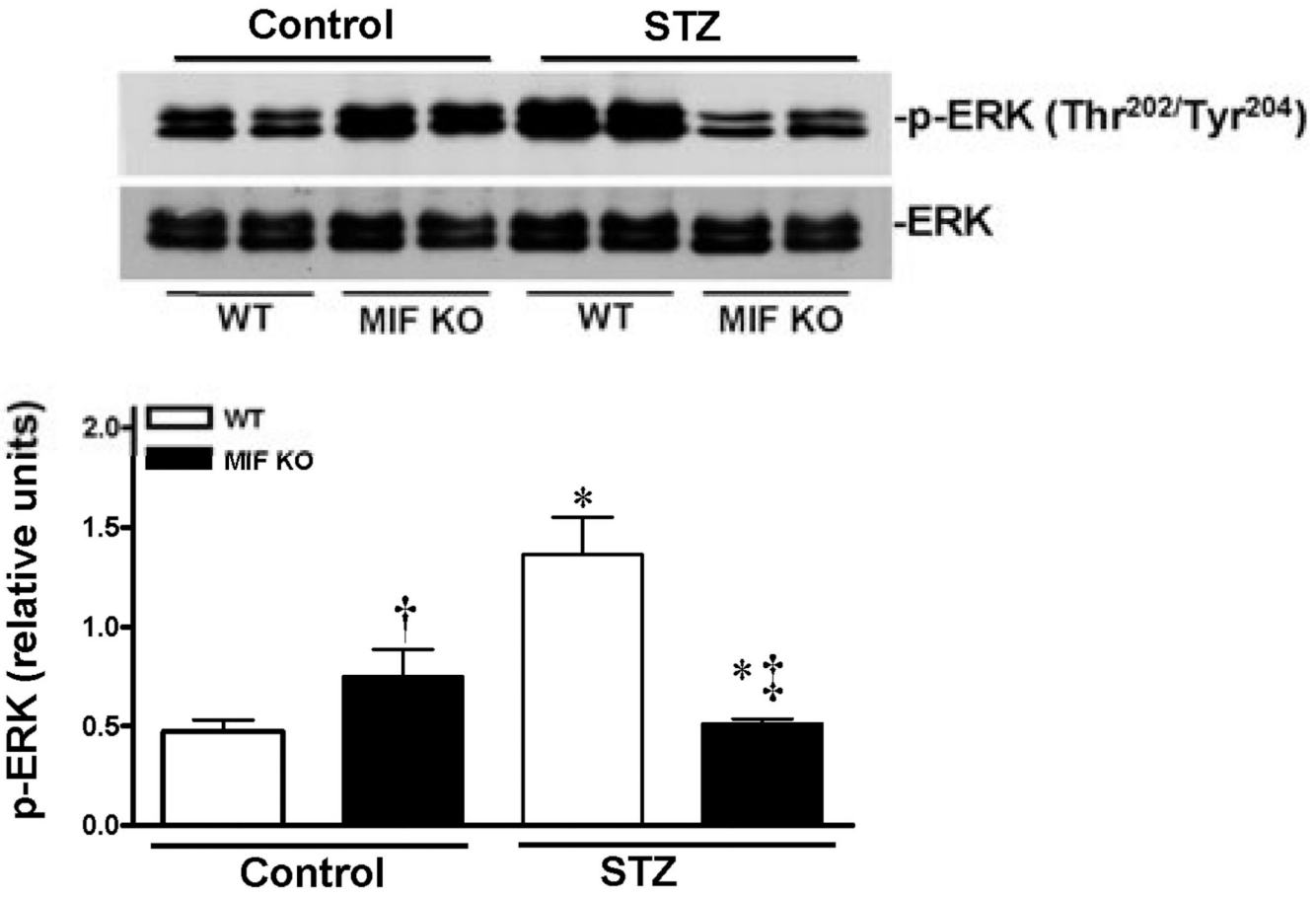

Figure 6.

STZ-induced T1D triggered ERK signaling pathway in the heart. Left ventricles from WT and MIF KO mice treated with or without STZ (200 mg/kg, i.p.) were used for making homogenates. Representative immunoblots of p-ERK and total ERK (upper panel), bars show the relative level of p-ERK (lower panel) in the hearts. Mean ± SEM; n =4 samples per group, *p < 0.05 *vs.* control group, respectively; †p < 0.05 *vs.* WT control; ‡p<0.05 *vs.* WT-STZ.

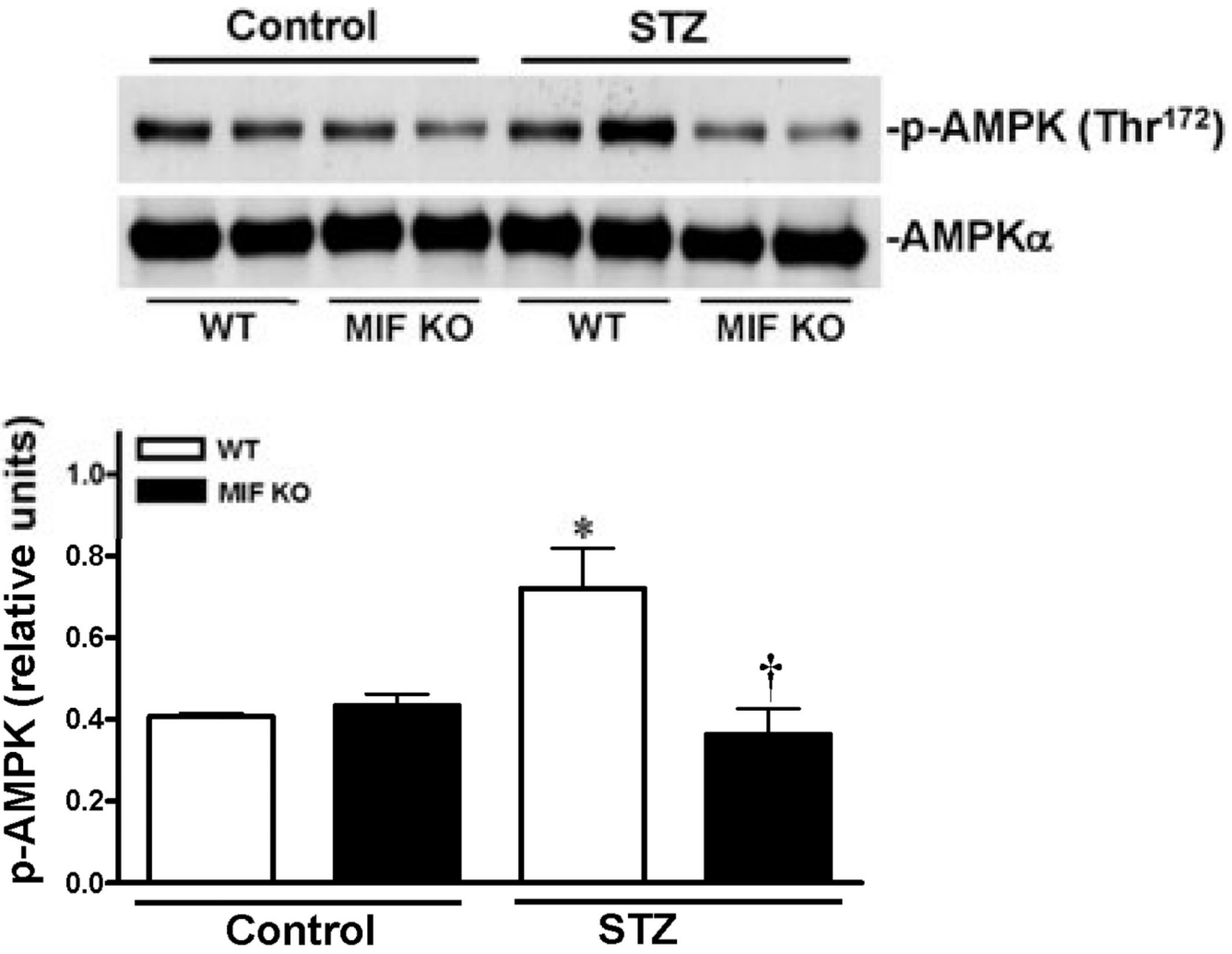

Figure 7.

Cardiac AMPK signaling pathway was up-regulated during STZ-induced T1D. Left ventricles from WT and MIF KO mice treated with or without STZ (200 mg/kg, i.p.) were used for making homogenates. Representative immunoblots of p-AMPK (Thr172) and total AMPK (upper panel), bars show the relative level of p-AMPK (lower panel) in the hearts. Mean ± SEM; n =4 samples per group, *$p < 0.05$ *vs.* control group, respectively; †$p < 0.05$ *vs.* WT-STZ.